Enantioselective Energy Transfer-Enabled Cyclization using a Privileged Al-Salen Photocatalyst

Julia Soika[1]†, Carina Onneken[1]†, Thorben Wiegmann[1,2], Tobias Morack[1,3], Leander Lindfeld[1], Marian Hebenbrock[4], Christian Mück-Lichtenfeld[1,2], Johannes Neugebauer[1,2]* & Ryan Gilmour[1]*

[1] Institute for Organic Chemistry, University of Münster; Corrensstraße 36, 48149 Münster (Germany)
[2] Center for Multiscale Theory and Computation, University of Münster; Corrensstraße 36, 48149 Münster (Germany)
[3] Institute for Organic Chemistry, University of Heidelberg, Im Neuenheimer Feld 270, 69120 Heidelberg (Germany)
[4] Institute for Inorganic and Analytical Chemistry, University of Münster; Corrensstraße 28/30, 48149 Münster (Germany)

*Corresponding authors. Email: j.neugebauer@uni-muenster.de; ryan.gilmour@uni-muenster.de
† These authors contributed equally to this work.

Abstract: Chiral catalysts that can engage multiple substrates, via distinct activation modes, to deliver enantioenriched products with high levels of fidelity are often described as *"privileged"*.[1] Antipodal to enzymatic specificity,[2] this generality enables the reactivity - selectivity divide in ground state landscapes to be effectively reconciled. Achieving this latitude in excited state paradigms remains a frontier, and efforts to identify privileged chiral photocatalysts are currently a core area of research. Aluminum salen complexes are emergent contenders on account of their well-defined photophysical properties and competence in photo-induced single electron transfer processes: this has recently been leveraged in the deracemization of cyclopropyl ketones.[3] To expand the activation repertoire of Al-salen photocatalysts, an unprecedented enantioselective energy transfer (EnT)[4] catalysis-enabled photocyclization of acrylanilides has been developed. This operationally simple strategy allows reactivity and enantioselectivity to be simultaneously regulated by an inexpensive, commercial chiral Al-salen complex upon irradiation at λ = 400 nm: this allows diverse cyclic products to be forged with high levels of enantioselectivity (up to 96:4 *e.r.*). Establishing this dichotomy in excited state activation modes serves to consolidate the privileged status of chiral Al-salen complexes in enantioselective photocatalysts and to complement their ubiquity in ground-state regimes.[5]

Introduction: Reconciling the juxtaposition of selectivity and generality is a recurrent challenge in enantioselective small molecule catalysis.[6] Driven by the socio-economic importance of this technology,[7-9] this division has been bridged by a growing portfolio of versatile chiral catalysts that operate across a broad spectrum of transformations.[10] Whilst successful catalyst blueprints are often bio-inspired,[11] enabling functional promiscuity in a manner antipodal to enzymatic specificity has been a key driver of innovation (see Figure 1, A): this creates the latitude necessary to rapidly penetrate new areas of chemical space (see Figure 1, B).[12] Orchestrated by well-defined architectures and substrate activation modes, enantioselectivity can often be rationalized *a priori*, thereby consolidating the status of these privileged actors in precision synthesis (see Figure 1, C). Whilst the notion of *"privileged catalysts"* is common in ground state reactivity,[13] extrapolating this conceptual paradigm to excited state enantioselective scenarios represents a challenge in asymmetric synthesis.[14-17] Advancing this field requires new structure - activation guidelines to be delineated[18,19] that reflect the energetic realities of asymmetric processes in which reactivity and chirality transfer occur in non-ground state scenarios.[20,21] The renaissance of organic

photochemistry provides an exciting opportunity to repurpose inexpensive, privileged chiral catalysts to simultaneously regulate reactivity and enable asymmetric induction in the presence of light as an external stimulus.[22,23]

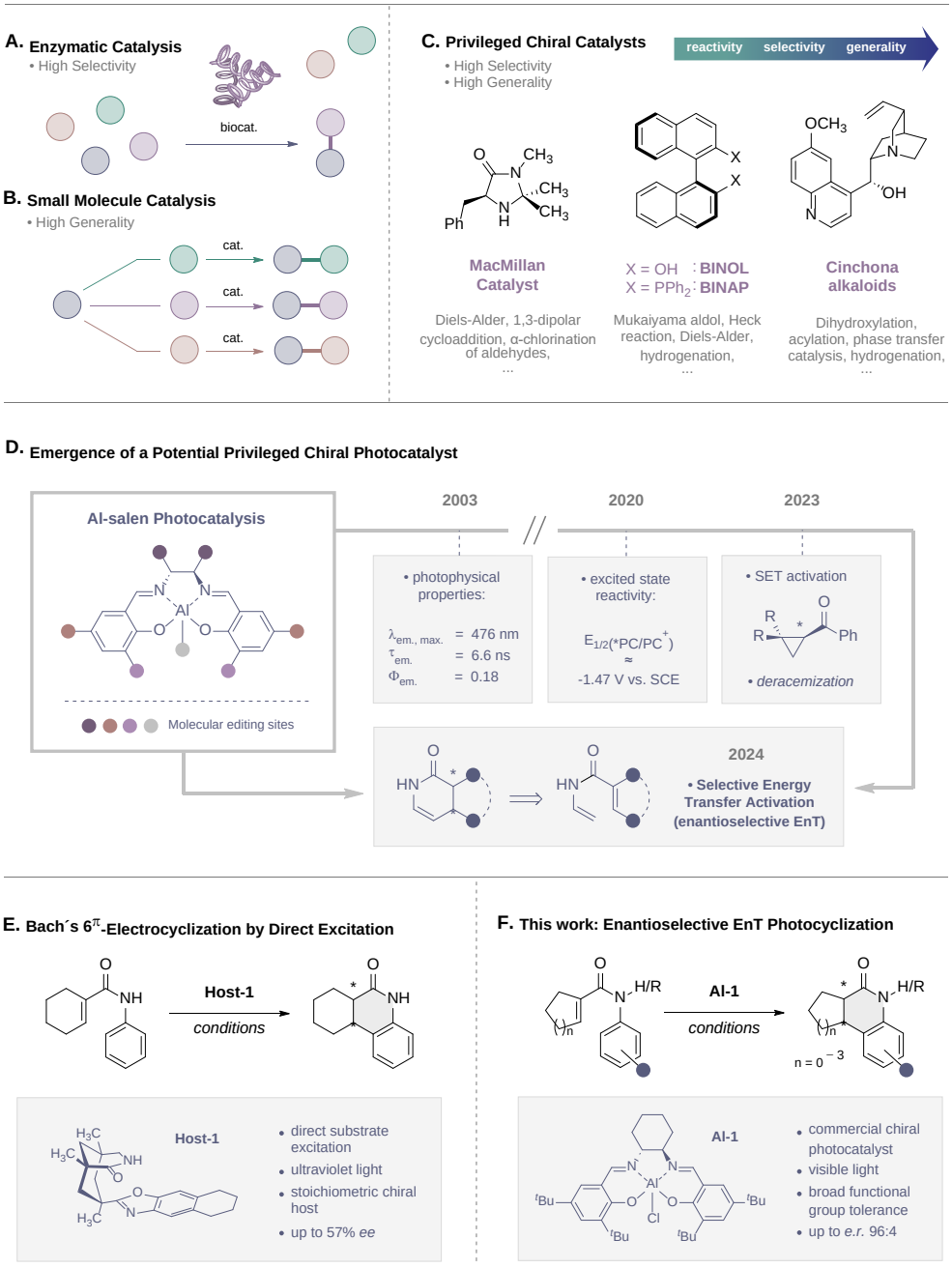

Fig 1: Generality of aluminum salen photocatalysis. A. Selectivity of enzymatic catalysis. **B.** Generality of small molecule catalysis. **C.** Ground state privileged chiral catalysts combine selectivity and generality. **D.** Emergence of Al-salen complexes as potential privileged chiral photocatalysts. **E.** 6π-Electrocyclization by direct excitation. **F.** This work: Enantioselective cyclization using an Al-salen photocatalyst.

Foundational examples from the groups of Bach,[24-26] Yoon,[27-28] and Meggers[29-30] have propelled the development of enantioselective photocatalysis using substrate – catalyst ensembles that are appointed with specific recognition units. To compliment these precision molecular design strategies, we recently validated C_2-symmetric aluminum salen complexes as efficient chiral photocatalysts for the deracemization of cyclopropanes via photo-induced single electron transfer (SET, see Figure 1, D).[3] The success of these inexpensive chiral complexes is grounded in their favorable photophysical properties, which include photon absorption in the visible range of the electromagnetic spectrum, comparably high excited state lifetimes, and the capacity to transfer a single electron upon excitation.[31-33] Given the transformative impact of C_2-symmetric metal salen complexes in asymmetric catalysis,[34-37] and in particular Al-salen complexes by Jacobsen and co-workers,[38-41] extending their repertoire to exited state reactions would be highly enabling. However, this requires generality to be established, and validation that chiral Al-salen complexes can effectively catalyze enantioselective excited state processes via discrete activation modes. To compliment the recent report of photo-induced single electron-transfer,[3] evidence of enantioselective energy transfer catalysis[42] using Al-salen- complexes would be a persuasive argument towards this objective. To that end, the development of a highly enantioselective cyclization of simple acrylanilides was developed under the auspices of Al-salen photocatalysis (see Figure 1, D). This transformation was inspired by the early work of Cleveland and Chapman,[43] and a seminal report by Bach and co-workers (see Figure 1, E)[44] describing the 6π-electrocyclization of a single acrylanilide by direct excitation in the UV range (λ = 300 nm) in the presence of super-stoichiometric chiral host (57% *ee*). Key to our reaction design was the premise that, upon irradiation with visible light, efficient energy transfer from the excited state Al-salen to the substrate would enable a photocyclization event (see Figure 1, F). Moreover, it was envisaged that Lewis coordination between the oxygen of the amide substrate and the central aluminum of the catalyst in the excited state would ensure that ring closure occurred within the confinement of the highly pre-organized, chiral environment to deliver optically enriched products. In a broader sense, this approach would contribute to the current interest in enantioselective photocyclization reactions. Elegant studies by Smith and co-workers have demonstrated that combining an Ir(III) photosensitizer with a chiral Lewis acid complex can enable this challenging transformation.[45] Furthermore, Yoon and colleagues have leveraged a precision hydrogen-bonding interaction between an Ir(III) catalyst and the substrate to render 6π photoelectrocyclizations highly enantioselective.[46]

Results & Discussion

To explore the feasibility of an enantioselective cyclization enabled by energy transfer photocatalysis, substrate **1a** bearing an unprotected amide was exposed to 10 mol% of commercially available aluminum salen complex **Al-1** under irradiation at 400 nm (violet light) in dichloromethane (see Figure 2, entry 1). Gratifyingly, the products *trans*- and *cis*-**2a** were obtained in a combined yield of 44% with enantioenrichement observed for both diastereomers (*trans*-**2a**: 74:26 enantiomeric ratio (e.r.), *cis*-**2a**: 68:32 e.r.). The diastereomeric ratio (d.r.) of 71:29 favored formation of the *trans*-product under these reaction conditions. Based on mechanistic investigations by Bach and co-workers,[44] it was evident that the enantiodetermining step (β to the carbonyl) was efficiently regulated by the photocatalyst: Competing protonation / H-shift pathways then account for the formation of two diastereomers. Encouraged by this initial result, the impact of structural and electronic changes at the editing site shown in Figure 2 was investigated (for a full catalyst screen see the Supplementary Information, Table S1). Removal of either substituent of the salicylidene ring (catalysts **Al-2** to **Al-4**) led to significant improvements in cyclization efficiency (up to 95%, entry 2) but at the expense of enantioselectivity (*trans*-**2a**: 63:37 e.r., *cis*-**2a**: 55:45 e.r., entry 2). In contrast, augmenting the steric bias of one substituent from *tert*-butyl to adamantyl (catalyst **Al-5**, entry 5) led to enhanced enantiomeric ratios of 84:16 (*trans*-**2a**) and 80:20 (*cis*-**2a**), albeit with a reduced yield of 15%. The introduction of catalyst **Al-6** with a modified backbone (from cyclohexyl to phenyl groups, entry 6) inhibited both the yield (14%) and selectivity (*trans*-**2a**: 65:35 e.r., *cis*-**2a**: 54:46

e.r.). Finally, changing the apical ligand from chloride to an oxygen-bridged dimeric structure (**Al-7**, entry 7) or a methyl group (**Al-8**, entry 8) had very marginal effects on enantioselectivity but led to notable reductions in yields (42% and 36%, respectively). These data allowed further reaction optimization to be conducted with the commercial catalyst **Al-1**, beginning with a study of the impact of the reaction medium (for a full solvent screen see Supplementary Information, Table S2). Reactions performed in acetone led to the formation of trace amounts of product (entry 9), whilst in acetonitrile (MeCN, entry 10) and toluene (entry 11) reduced yields (33% both) and enantioselectivities were observed (*trans*-**2a**: 64:36 e.r., *cis*-**2a**: 62:38 e.r. and *trans*-**2a**: 64:36 e.r., *cis*-**2a**: 56:44 e.r., respectively).

The addition of nBu$_4$NCl had a beneficial effect on the reaction outcome[47] (for a detailed screen of additives see the Supplementary Information, Table S3) (entry 12), and its addition allowed **2a** to be generated in 67% with a d.r. of 67:33 (*trans*:*cis*), and with encouraging enantiomeric ratios of 78:22 (*trans*-**2a**) and 80:20 (*cis*-**2a**). In the presence of hexafluoroisopropanol (HFIP, entry 13), product **2a** was formed almost quantitatively (95%) with an equimolar ratio of diastereomers (51:49 *trans*:*cis*): the enantioselectivity was lower (67:33 e.r.) for both diastereomers. The reaction with nBu$_4$NCl was repeated at -20 °C (entry 14) and improved enantiomeric ratios of 82:18 (*trans*-**2a**) and 85:15 (*cis*-**2a**) could be achieved. The addition of a drying agent to reactions run at low temperatures proved to be pivotal, and the simple addition of molecular sieves (MS, entry 15) led to a notable improvement in yield without adversely affecting the enantioselectivity. Finally, increasing the catalyst loading and reducing the amount of molecular sieves enabled product **2a** to be generated in 67% [84:16 (*trans*-**2a**) and 90:10 (*cis*-**2a**, entry 17)].

Having identified optimized reaction conditions, the scope of the transformation was investigated (see Figure 3, for an extended scope and limitations see the Supplementary Information, Figures S1 and S2). Gratifyingly, this enantioselective photocyclization catalyzed by Al-salen **Al-1** proved to be compatible with secondary (**2a**) and tertiary amides, which complements methods that require *N*-substitution.[45,46] To explore the influence of changes to the aryl ring of the acrylanilide, *para*-substituted substrates (**2b** – **2h**) were investigated: these substrates proved to be compatible with the reaction conditions. In all cases, synthetically useful enantiomeric ratios were obtained for both diastereomers, with formation of the *trans*-products being favored.

Halogen- (**2b**/**c**) and alkyl-substituents (**2d**/**e**) were tolerated, and enantioselectivities of up up to 94:6 e.r. for *cis*-**2d** could be obtained. The broad functional group tolerance of the transformation is reflected in the formation of silylated (**2f**/**g**, up to 94:6), and borylated adducts [up to e.r. 90:10 & 93:7 (*trans*- and *cis*-**2h**, respectively)]. Decreasing or increasing the ring size of the cyclic olefin was also tolerated and enabled products **2i** and **2j** to be generated. In the case of *cis*-**2j**, the optical purity could be improved by facile recrystallization; this served a secondary purpose in enabling the absolute configuration of *cis*-**2j** to be assigned as (2a*S*,8b*R*) (see insert in Figure 3, CCDC number 2368374). Finally, product **2k** possessing a quaternary stereocenter could be formed from the tetra-substitued alkene precursor in 95% yield with e.r. 81:19 for the *trans*-diastereomer, which was the major product. In the case of more challenging substrates such as **1l** and **1n**, the enantioselectivity could be improved by up to 15% by *N*-methylation through enhanced structural pre-organization prior to cyclization. This enabled tricycles **2m** and **2o** to be forged in 97% and quantitative yield, respectively. Consistently high levels of enantioselectivity were observed for both diastereomeric sets (*trans*-**2m** 96:4 and *cis*-**2m** 93:7; *trans*-**2o** 96:4 and *cis*-**2o** 91:9).

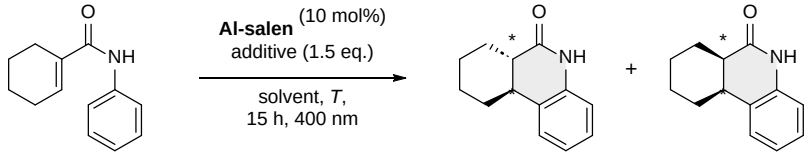

1a *trans*-**2a** *cis*-**2a**

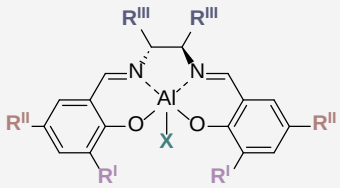

Al-1: R^{I}: ^{t}Bu; R^{II}: ^{t}Bu; R^{III}: -$(CH_2)_2$-; X: Cl
Al-2: R^{I}: H; R^{II}: ^{t}Bu; R^{III}: -$(CH_2)_2$-; X: Cl
Al-3: R^{I}: ^{t}Bu; R^{II}: H; R^{III}: -$(CH_2)_2$-; X: Cl
Al-4: R^{I}: Ph; R^{II}: H; R^{III}: -$(CH_2)_2$-; X: Cl
Al-5: R^{I}: Ad; R^{II}: Me; R^{III}: -$(CH_2)_2$-; X: Cl
Al-6: R^{I}: ^{t}Bu; R^{II}: ^{t}Bu; R^{III}: Ph; X: Cl
Al-7: R^{I}: ^{t}Bu; R^{II}: ^{t}Bu; R^{III}: -$(CH_2)_2$-; X: O-Al(salen)
Al-8: R^{I}: ^{t}Bu; R^{II}: ^{t}Bu; R^{III}: -$(CH_2)_2$-; X: Me

Entry	Catalyst	Solvent	Additive (1.5 eq.)	*T* [°C]	yield **2a** [%]	*d.r.* (*trans*:*cis*)	*e.r. trans*	*e.r. cis*
1	**Al-1**	DCM	-	r.t.	44	71:29	74:26	68:32
2	**Al-2**	DCM	-	r.t.	95	55:45	63:37	55:45
3	**Al-3**	DCM	-	r.t.	64	64:36	67:33	53:47
4	**Al-4**	DCM	-	r.t.	83	63:37	67:33	57:43
5	**Al-5**	DCM	-	r.t.	15	66:34	84:16	80:20
6	**Al-6**	DCM	-	r.t.	14	71:29	65:35	54:46
7	**Al-7**	DCM	-	r.t.	42	67:33	23:77	27:73
8	**Al-8**	DCM	-	r.t.	36	71:29	73:27	75:25
9	**Al-1**	acetone	-	r.t.	< 5	n.d.	n.d.	n.d.
10	**Al-1**	MeCN	-	r.t.	33	56:44	64:36	62:38
11	**Al-1**	toluene	-	r.t.	33	67:33	64:36	56:44
12	**Al-1**	DCM	*n*Bu_4NCl	r.t.	67	67:33	78:22	80:20
13	**Al-1**	DCM	HFIP	r.t.	95	51:49	67:33	67:33
14[a]	**Al-1**	DCM	*n*Bu_4NCl	-20	50	64:36	82:18	85:15
15[a,b]	**Al-1**	DCM	*n*Bu_4NCl MS (3 Å)	-20	55	62:38	82:18	88:12
16[a,b,c]	**Al-1**	DCM	*n*Bu_4NCl MS (3 Å)	-20	57	66:34	84:16	90:10
17[a,c,d]	**Al-1**	DCM	*n*Bu_4NCl MS (3 Å)	-20	67	66:34	84:16	90:10

Fig 2: Optimization of the reaction conditions for the enantioselective photocyclization of 1a. Unless stated otherwise, reactions were performed with **1a** (0.1 mmol), **Al-salen catalyst** (10 mol%) and additive (1.5 eq.) in DCM under an argon atmosphere. Irradiation took place at 400 nm, for irradiation at -20 °C a glass rod was used as an optical guiding rod. Isolated yields of combined *trans*- and *cis*-**2a** are reported. The d.r. was determined by ^{1}H NMR spectroscopy; the e.r. was determined by high-performance liquid chromatography (HPLC) analysis on a chiral stationary phase. a) Reactions at -20 °C were run for 21 h; b) 15 mg of molecular sieves were used; c) 20 mol% of catalyst was used; d) 6 mg of molecular sieves were used.

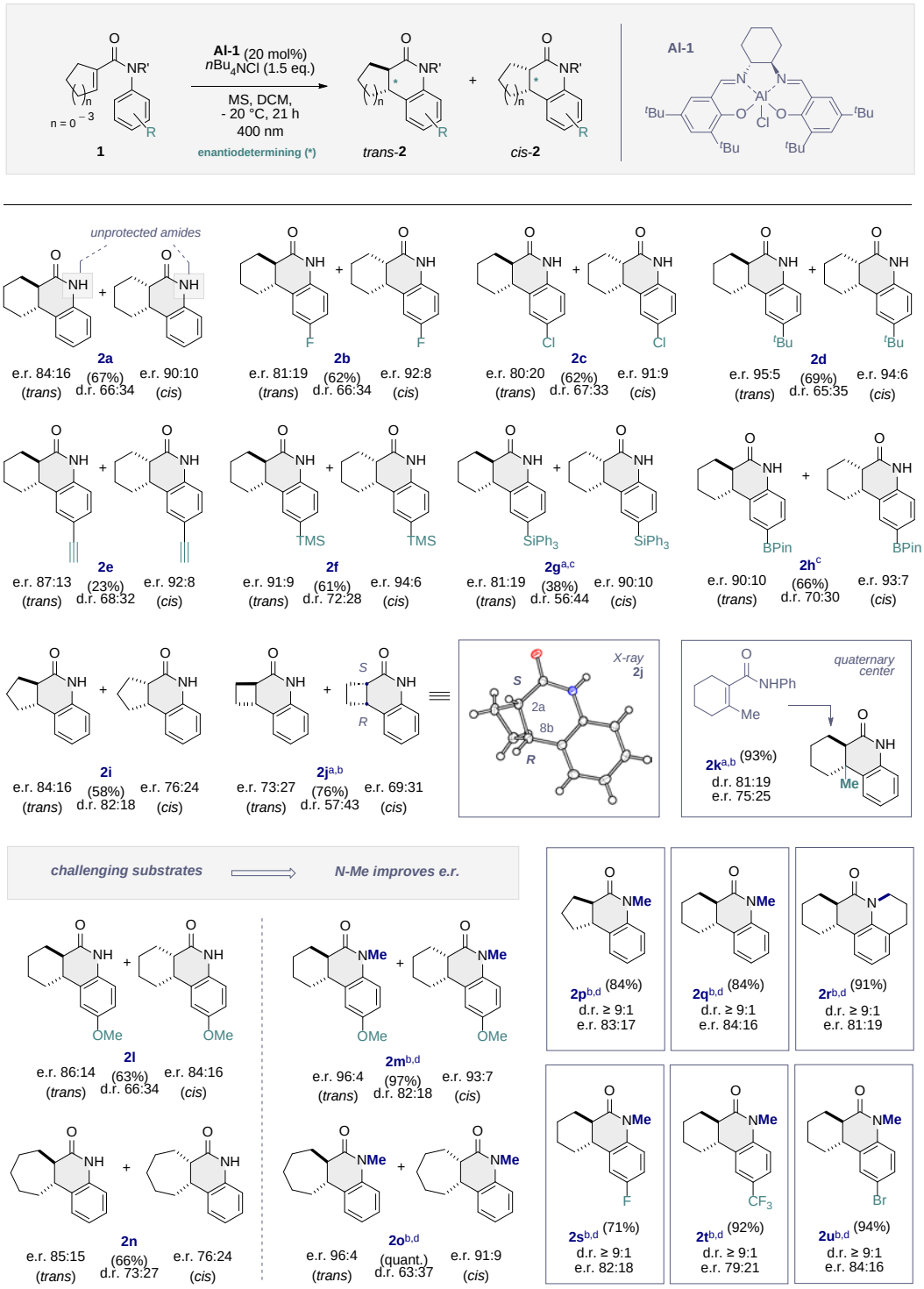

Fig 3: Scope of the enantioselective photocyclization. Unless stated otherwise, reactions were performed with substrate (0.1 mmol), **Al-1** (20 mol%), *n*Bu$_4$Cl (1.5 eq.) and molecular sieves (3 Å, 6 mg) in DCM under argon atmosphere. Reaction mixtures were irradiated at 400 nm and -20 °C for 21 h. Isolated yields of combined *trans*- and *cis*-products are reported. The d.r. was determined by ^{1}H NMR spectroscopy; the e.r. was determined by HPLC analysis on a chiral stationary phase. a) 65 h reaction time; b) HFIP (1.5 eq.) was used instead of *n*Bu$_4$NCl; c) irradiated at room temperature; d) irradiated at -40 °C.

To further expand this *N*-Me amide scope, revised reaction conditions were employed in which HFIP was applied as an additive instead of nBu$_4$NCl and reactions were performed at a lower temperature (-40 °C). This enabled the 5- and 6-membered adducts **2p** and **2q** to be generated, as well as a challenging tetracyclic adduct **2r** (91% yield, e.r. 81:19). It is interesting to note that the *trans*:*cis* selectivity was ≥ 9:1 in all cases. Introducing electron-withdrawing substituents to complement the methoxy-derivative **2m** was also successful as is illustrated by compounds **2s**-**2u** (up to 94% yield, d.r. ≥ 9:1, up to 84:16).

Attention was then turned towards mechanistic investigations to gain further insights into this enantioselective energy transfer process (Figure 4). Control reactions in the absence of catalyst **Al-1**, or shielded from light, did not lead to product formation but instead the starting material **1a** was recovered quantitatively (see Figure 4, A). Furthermore, no product was observed when **Al-1** was replaced with the salen ligand **Salen-1**, indicating that substrate coordination to the aluminum center is important in simultaneously regulating reactivity and selectivity. The lack of reactivity in the absence of the catalyst is further supported by UV/vis spectroscopy: only the catalyst absorbs electromagnetic radiation at 400 nm, while the absorption maximum of the substrate **1a** is located at ~260 nm (Figure 4, B). Titration of substrate **1a** to the catalyst did not cause a bathochromic shift of the absorption band ($\lambda_{max.} \approx 360$ nm) indicating that Lewis acid-base coordination between the catalyst and the substrate is not operational in the ground state. This was further verified by ^{13}C NMR spectroscopy (see the Supplementary Information for more details). Exploring the temperature-dependence of the reaction revealed the expected linear correlation between *ln*(e.r.) and the reciprocal of the temperature (Figure 4, C). To gain additional insight into the nature of the interaction between the excited state catalyst and the substrate, cyclic voltammetry of various substrates was performed. As is evident from Figure 4D, no reduction was observed for any of the substrates investigated in MeCN. Consequently, SET to the substrates is highly improbable, and a mechanism based on energy transfer from the catalyst in its triplet excited state is likely to be operational (Figure 4, E): this is further supported by computational investigations (*vide infra*). Following energy transfer, the excited substrate undergoes cyclization which is enantiodetermining. Subsequent intersystem crossing (ISC) leads to either a [1,5]-H shift or external protonation to furnish the final product diastereomers. To distinguish between these potential pathways, experiments with deuterated substrates **1v** and **1w** were conducted (Figure 4, F).

Replacement the phenyl ring of acrylanilide **1a** with a per-deuterated ring (substrate **1v**) led to high levels of deuterium incorporation at the 6a-position of *trans*-**2v** (84% D) whilst in *cis*-**2v** only 5% D-incorporation was observed. This suggests that a [1,5]-H shift is operative in the formation of the *trans*-systems, whereas the corresponding *cis*-diastereomers are formed via external protonation. To investigate the potential role of the solvent, the experiment was repeated in deuterated dichloromethane. Similar degrees of deuterium incorporation were observed, thereby excluding the solvent as a proton source. In the case of secondary amides, a potential hydrogen source is the unprotected amide. Therefore, further experiments were performed with deuterated substrate **1w** which contains a *N*-methyl group. In alignment with the previous observations, a higher level of deuterium incorporation was observed for *trans*-**2w** (55%) than for *cis*-**2w** (15%). Since the photocyclization of **1w** was facilitated by the addition of HFIP (*vide supra*), the possibility of this additive serving as a protonation agent was considered. Conducting the experiment with HFIP-OD led to a significant increase of deuterium incorporation, and this was especially pronounced in the *cis*-diastereomer: from 15% D with HFIP-OH to 53% D with HFIP-OD. Repeating the experiment with DCM-d_2 did not reveal a solvent influence but rather verified the initial results. These findings further substantiate the hypothesis that the *cis*-products arise primarily via external protonation, while a [1,5]-H shift dominates in the formation of the *trans*-diastereomers.

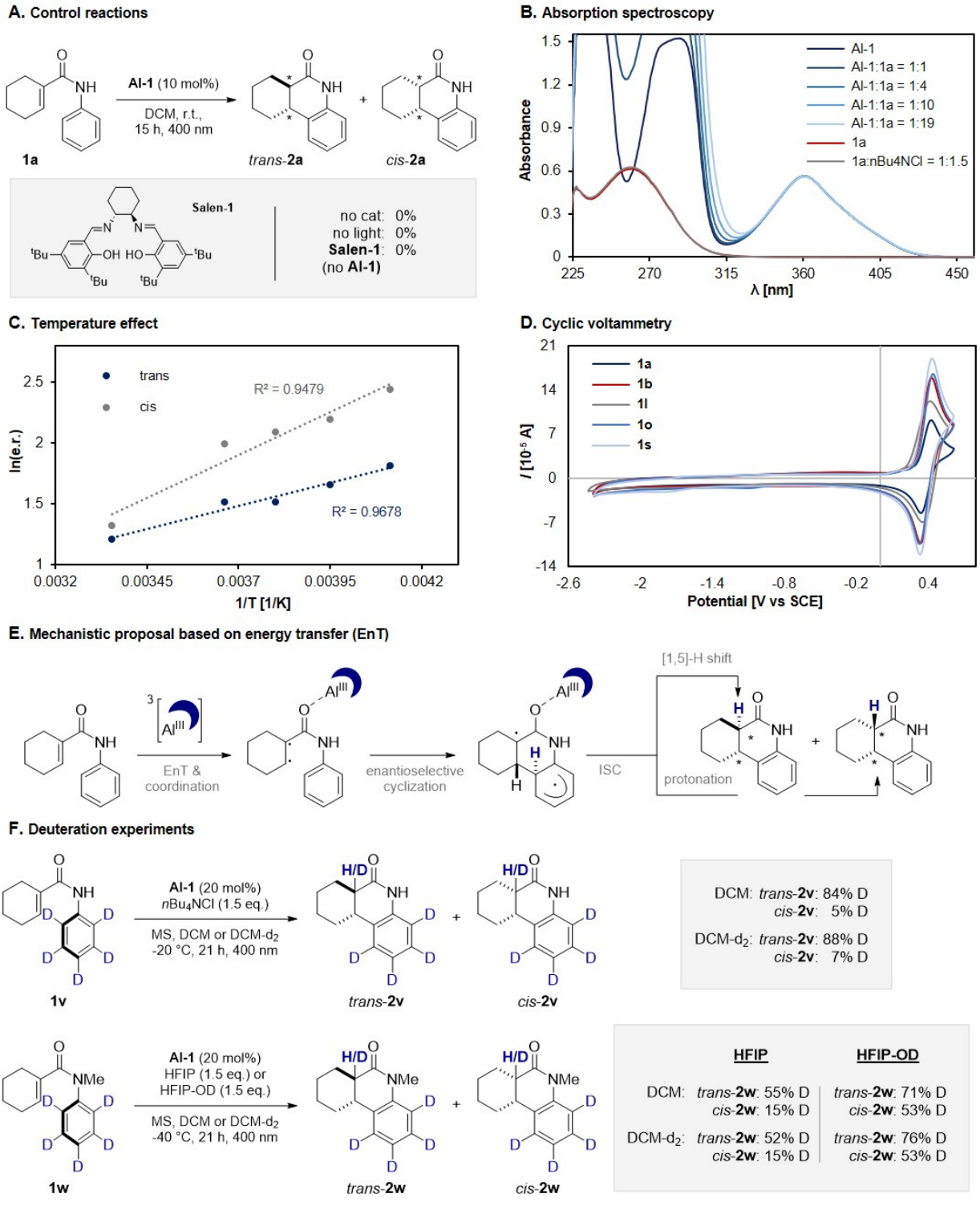

Fig 4: Mechanistic Investigations. A. Control reactions; reactions were performed on a 0.1 mmol scale. **B.** UV-vis absorption spectra of **1a** and **Al-1** (each: *c* = 0.05 mM in DCM) and mixtures. **C.** Effect of varying temperature on the e.r.; reactions were performed on a 0.1 mmol scale. **D.** Cyclic voltammograms of **1a**, **1b**, **1l**, **1o** and **1s** (in MeCN). **E.** A potential reaction mechanism for the photocyclization catalyzed by **Al-1**. **F.** Deuteration experiments; reactions were performed on a 0.1 mmol scale.

Further experiments applying non-deuterated substrates in combination with deuterated solvent and/or HFIP as the proton source are in line with the presented results (see the Supplementary Information for more details).

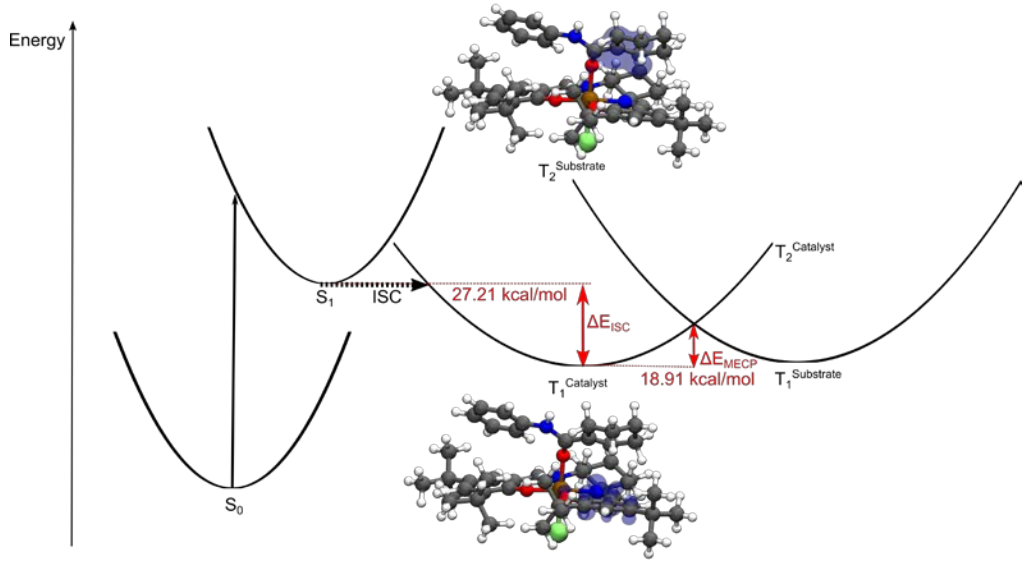

Figure 5: Reaction Mechanism. Schematic illustration of the proposed path across multiple potential energy surfaces from the photoexcitation to the triplet energy transfer (EnT).

To further support the involvement of an energy transfer mechanism, a detailed computational investigation was conducted: this enabled an electron transfer mechanism to be ruled unlikely. Calculation of ground and excited state redox potentials in acetonitrile at 25 °C, and in DCM at -20 °C, revealed a mismatch of 0.61 eV and 0.50 eV for the highest investigated excited state (S_1), respectively. The S_0 and T_1 redox potentials show a larger mismatch (see the Supplementary Information). Furthermore, the frontier molecular orbitals involved in the excitation show a significant localization solely on the catalyst which contradicts an electron transfer mechanism. In contrast, this investigation revealed that the postulated triplet energy transfer mechanism was plausible. Calculated triplet excitation-energy transfer couplings[48] for the complex studied (**Al-1-1a**) are about one order of magnitude larger than the couplings of the related complex which was shown to undergo electron transfer.[3] DFT calculations suggest a slight uphill energy transfer mechanism as the triplet energy of the catalyst is about 0.17 eV higher than the triplet energy of the substrate. Upon coordination with the acrylanilide, however, the energy of the catalyst-localized triplet state increases, while model calculations suggest that the energy of the substrate-localized triplet state within the complex decreases (see the Supplementary Information for details). Consequently, the energy gap between the two triplet states is further reduced. A CASSCF single-point calculation on the DFT minimum-energy structure of the (catalyst-localized) T_1 state revealed that the spin density in the T_2 state is localized on the substrate. This further supports the hypothesis of an uphill triplet energy transfer mechanism. A minimum energy crossing point (MECP) between these two states was calculated to obtain the molecular structure for the crossing into a substrate-localized triplet state. The molecular structure obtained shows little change in the minimum-energy structure of the catalyst-localized triplet state and the changes that are observed are in agreement with the expected motion along the reaction coordinate: This further supports the hypothesis of energy transfer. A Marcus-theory based approximation[49] revealed a barrier of 0.82 eV for the energy transfer. The energy released by relaxation after the intersystem crossing is in the same energy range. Based on these CASSCF and DFT calculations,

it is proposed that an uphill triplet energy transfer mechanism following the path schematically shown in Figure 5 as the most probable scenario: Following an initial excitation into the S_1 state of the catalyst we assume that an intersystem crossing to the catalyst-localized T_1 state occurs. This catalyst-localized state crosses with another substrate-localized triplet state, which becomes the lowest-energy triplet state beyond the crossing point. The energy barrier for this crossing can be overcome if the adiabatic energy difference of the S_1 and T_1 (ΔE_{ISC}) states is larger than the energy barrier to the minimum energy crossing point (ΔE_{MECP}).

Conclusions

To contribute to the privileged status of Al-salen complexes in asymmetric catalysis, a highly enantioselective photocyclization of simple acrylanilides mediated by triplet energy catalysis is disclosed. Validating this second photoactivation mode in asymmetric photocatalysis significantly expands the operational capabilities of these commercial, earth-abundant complexes and further cements their privileged status.

Acknowledgments

We gratefully acknowledge the support provided by the technical departments of the Institute for Organic Chemistry at the University of Münster. We thank the German Research Foundation [SFB 858, IRTG 2678 (GRK 2678-437785492) and SFB 1459 (CRC 1459-433682494)] for generous financial support.

Data Availability Statement

Data availability CCDC 2368376 (for ***rac*-2j-*trans***), 2368374 (for **2j-*cis***), 2368375 (for ***rac*-2n-*trans***) and 2368377 (for ***rac*-2k-*trans***) contains the supplementary crystallographic data for compound **1**. The data can be obtained free of charge from The Cambridge Crystallographic Data Centre [http://www.ccdc.cam.ac.uk/data_request/cif]. Supplementary Information is available for this paper. All data are available in the main text or the supplementary materials. Correspondence and requests for materials should be addressed to Prof. Ryan Gilmour (ryan.gilmour@uni-muenster.de).

References

1. Yoon, T. P.; Jacobsen, E. N. Privileged chiral catalysts. *Science* **2003**, *299*, 1691–1693.
2. Knowles, J. R. Enzyme catalysis: not different, just better. *Nature* **1991**, *350*, 121-124.
3. Onneken, C.; Morack, T.; Soika, J.; Sokolova, O.; Niemeyer, N.; Mück-Lichtenfeld, C.; Daniliuc, C. G.; Neugebauer, J.; Gilmour, R. Light Enabled Deracemization of Cyclopropanes by Al Salen Photocatalysis. *Nature* **2023**, *621*, 735-759.
4. Neveselý, T.; Wienhold, M.; Molloy, J. J.; Gilmour, R. Advances in the *E* → *Z* Isomerization of Alkenes using Small Molecule Photocatalysts. *Chem. Rev.* **2022**, *122,* 2650-2694.
5. Shaw, S.; White, J. D. Asymmetric Catalysis Using Chiral Salen-Metal Complexes: Recent Advances. *Chem. Rev.* **2019***, 119*, 9381–9426.
6. Jacobsen, E. N.; Pfaltz, A.; Yamamoto, H. *Comprehensive asymmetric catalysis.* 1st ed. (Springer, London, **1999**).
7. Mitchison, A.; Finkelstein, J. Small-molecule catalysis. *Nature* **2008**, *255*, 303.
8. Wender, P. A.; Miller, B. L. Synthesis at the molecular frontier. *Nature* **2009**, *460*, 197-201.
9. *Asymmetric Catalysis in Industrial Scale: Challenges, Approaches and Solutions*, 2nd ed., (Ed. Blaser, H.-U.; Federsel, H.-J.) Wiley: Weinheim (**2010**).

10. Trost, B. M. Atom economy-a challenge for organic synthesis: homogeneous catalysis leads the way. *Angew. Chem. Int. Ed.* **1995**, *34*, 259-281.
11. Knowles, R. R.; Jacobsen, E. N. Attractive noncovalent interactions in asymmetric catalysis: Links between enzymes and small molecule catalysts. *Proc. Natl. Acad. Sci. U. S. A.* **2010**, *107*, 20678-20685.
12. Kirkpatrick, P.; Ellis, C. Chemical Space. *Nature* **2004**, *432*, 823.
13. Privileged Chiral Ligands and Catalysts (Ed. Zhou, Q.-L.), Wiley-VCH Verlag GmbH & Co. KGaA (**2011**).
14. Seebach, D. Organic Synthesis—Where now? *Angew. Chem. Int. Ed.* **1990***, 29*, 1320–1367.
15. Prier, C. K.; Rankic, D. A.; MacMillan, D. W. C. Visible light photoredox catalysis with transition metal complexes: applications in organic synthesis. *Chem. Rev.* **2013***, 113*, 5322–5363.
16. Silvi, M.; Melchiorre, P. Enhancing the potential of enantioselective organocatalysis with light. *Nature* **2018***, 554,* 41–49.
17. Genzink, M. J.; Kidd, J. B.; Swords, W. B.; Yoon, T. P. Chiral Photocatalyst Structures in Asymmetric Photochemical Synthesis. *Chem. Rev.* **2022**, *122*, 1654–1716.
18. Balcells, D.; Clot, E.; Eisenstein, O.; Nova, A; Perrin, L. Deciphering Selectivity in Organic Reactions: A Multifaceted Problem. *Acc. Chem. Res.* **2016**, *49*, 1070–1078.
19. Betinol, I. O.; Lai, J.; Thakur, S.; Reid, J. P. A Data-Driven Workflow for Assigning and Predicting Generality in Asymmetric Catalysis. *J. Am. Chem. Soc*. **2023**, *145*, 12870-12883.
20. Arias-Rotondo, D. M.; McCusker, J. K. The photophysics of photoredox catalysis: a roadmap for catalyst design. *Chem. Soc. Rev.* **2016**, *45*, 5803–5820.
21. Hammond, G. S.; Cole, R. S. Asymmetric Induction during Energy Transfer. *J. Am. Chem. Soc.* **1965**, *87*, 3256–3257.
22. Stoll, R. S.; Hecht, S. Artificial light-gated catalyst systems. *Angew. Chem. Int. Ed.* **2010**, *49*, 5054–5075.
23. Kathan, M.; Hecht, S. Photoswitchable molecules as key ingredients to drive systems away from the global thermodynamic minimum. *Chem. Soc. Rev.* **2017**, *46*, 5536–5550.
24. Bach, T.; Bergmann, H.; Grosch, B.; Harms, K. Highly enantioselective intra- and intermolecular 2 + 2 photocycloaddition reactions of 2-quinolones mediated by a chiral lactam host: host-guest interactions, product configuration, and the origin of the stereoselectivity in solution. *J. Am. Chem. Soc.* **2002**, *124*, 7982–7990.
25. Tröster, A.; Alonso, R.; Bauer, A.; Bach, T. Enantioselective Intermolecular 2 + 2 Photocycloaddition Reactions of 2(1H)-Quinolones Induced by Visible Light Irradiation. *J. Am. Chem. Soc.* **2016**, *138*, 7808–7811.
26. Bauer, A.; Westkämper, F.; Grimme, S.; Bach, T. Catalytic enantioselective reactions driven by photoinduced electron transfer. *Nature* **2005**, *436*, 1139–1140.
27. Skubi, K. L. *et al.* Enantioselective Excited-State Photoreactions Controlled by a Chiral Hydrogen-Bonding Iridium Sensitizer. *J. Am. Chem. Soc.* **2017**, *139*, 17186–17192.
28. Kidd J. D. *et al.* Enantioselective Paternò-Büchi Reactions: Strategic Application of a Triplet Rebound Mechanism for Asymmetric Photocatalysis. *J. Am. Chem. Soc*. **2024**, *146*, 15293-15300.
29. Huo, H. *et al.* Asymmetric photoredox transition-metal catalysis activated by visible light. *Nature* **2014**, *515*, 100–103.
30. Zhang, C *et al.* Catalytic α-Deracemization of Ketones Enabled by Photoredox Deprotonation and Enantioselective Protonation. *J. Am. Chem. Soc*. **2021**, *143*, 13393-13400.
31. Baleizão, C. *et al.* Photochemistry of chiral pentacoordinated Al salen complexes. Chiral recognition in the quenching of photogenerated tetracoordinated Al salen transient by alkenes. *Photochem. Photobiol. Sci.* **2003**, *2*, 386–392.
32. Cozzi, P. G. *et al.* Photophysical properties of Schiff-base metal complexes. *New J. Chem.* **2003***, 27*, 692–697.

33. Gualandi, A. *et al.* Aluminum(III) Salen Complexes as Active Photoredox Catalysts. *Eur. J. Org. Chem.* **2020**, 1486–1490.
34. Zhang, W.; Loebach, J. L.; Wilson, S. R.; Jacobsen, E. N. Enantioselective epoxidation of unfunctionalized olefins catalyzed by salen manganese complexes. *J. Am. Chem. Soc.* **1990**, *112*, 2801–2803.
35. Jacobsen, E. N.; Zhang, W.; Muci, A. R.; Ecker, J. R.; Deng, Li. Highly enantioselective epoxidation catalysts derived from 1,2-diaminocyclohexane. *J. Am. Chem. Soc.* **1991**, *113*, 7063-7064.
36. Irie, R.; Noda, K.; Ito, Y.; Matsumoto, N.; Katsuki, T. Catalytic asymmetric epoxidation of unfunctionalized olefins using chiral (salen)manganese(III) complexes. *Tetrahedron: Asymmetry* **1991**, *2*, 481–494.
37. Steinlandt, P. S.; Zhang, L.; Meggers, E. Metal Stereogenicity in Asymmetric Transition Metal Catalysis. *J. Am. Chem. Soc.* **2023**, *123*, 4764-4794.
38. Sigman, M. S.; Jacobsen, E. N. Enantioselective Addition of Hydrogen Cyanide to Imines Catalyzed by a Chiral (Salen)Al(III) Complex. *J. Am. Chem. Soc*. **1998**, *120*, 5315-5316.
39. Myers, J. K.; Jacobsen, E. N. Asymmetric Synthesis of β-Amino Acid Derivatives via Catalytic Conjugate Addition of Hydrazoic Acid to Unsaturated Imides. *J. Am. Chem. Soc*. **1999**, *121*, 8959–8960.
40. Taylor, M. S.; Jacobsen, E. N. Enantioselective Michael Additions to α,β-Unsaturated Imides Catalyzed by a Salen-Al Complex. *J. Am. Chem. Soc*. **2003**, *125*, 11204–11205.
41. Vanderwal, C. D.; Jacobsen, E. N. Enantioselective Formal Hydration of α,β-Unsaturated Imides by Al Catalyzed Conjugate Addition of Oxime Nucleophiles. *J. Am. Chem. Soc.* **2004**, *126*, 14724–14725.
42. Großkopf, J.; Kratz, T.; Rigotti, T.; Bach, T. Enantioselective Photochemical Reactions Enabled by Triplet Energy Transfer. *Chem. Rev.* **2022***, 122*, 1626–1653.
43. Cleveland, P. G.; Chapman, O. L. Non-oxidative photocyclization of alkyl-substituted acrylic acid anilides to dihydrocarbostyrils. *Chem. Commun.* **1967**, 1064−1065.
44. Bach, T.; Grosch, B.; Strassner, T.; Herdtweck, E. Enantioselective [6π]-Photocyclization Reaction of an Acrylanilide Mediated by a Chiral Host. Interplay between Enantioselective Ring Closure and Enantioselective Protonation. *J. Org. Chem*. **2003**, *68*, 1107-1116.
45. Jones, B. A.; Solon, P.; Popescu, M. V.; Du, J.-Y.; Paton, R.; Smith, M. D. Catalytic Enantioselective 6π Photocyclization of Acrylanilides. *J. Am. Chem. Soc.* **2023**, *145*, 171–178.
46. Swords, W. B.; Lee, H.; Park, Y.; Llamas, F.; Skubi, K. L.; Park, J.; Guzei, I. A.; Baik, M.-H.; Yoon, T. P. Highly Enantioselective 6π Photoelectrocyclizations Engineered by Hydrogen Bonding. *J. Am. Chem. Soc.* **2023**, *145*, 27045–270543.
47. Tazuke, S.; Kitamura, N.; Kawanishi, Y. Problems of back electron transfer in electron transfer sensitization. *J. Photochem.* **1985***, 29*, 123–138.
48. Käfer, S.; Niemeyer, N.; Tölle, J.; Neugebauer, J. Triplet Excitation-Energy Transfer Couplings from Subsystem Time-Dependent Density-Functional Theory. *J. Chem. Theory Comput.* **2024**, *20*, 2475–2490.
49. Solé-Daura, A.; Maseras, F. Straightforward computational determination of energy-transfer kinetics through the application of the Marcus theory. *Chem. Sci.* **2024**, *15*, 13650–13658.